Experimental and Quantum Study of Adsorption of Ozone (O_3) on Amorphous Water Ice Film

F. Borget, T. Chiavassa,* A. Allouche, and J. P. Aycard

Physique des Interactions Ioniques et Moléculaires, Université de Provence et CNRS, UMR 6633, Boîte 542, Centre de St. Jérôme, F-13397 Marseille, Cedex 20, France

Received: May 12, 2000; In Final Form: July 28, 2000

Ozone (O_3) adsorption and desorption on amorphous water ice film is monitored by Fourier transform infrared spectroscopy (FTIR) using the temperature-programmed desorption (TPD) method. A single type of site is observed between O_3 and ice which involves the dangling OH bonds of the amorphous ice. The O_3 desorption occurs between 70 and 90 K and the associated desorption energy is 20 kJ/mol. This value is in good agreement with that estimated from Periodic Hartree−Fock (PHF) calculations using a density functional theory (DFT) evaluation of the electronic correlation energy. These calculations confirmed the electrostatic nature of the interaction forces. The dangling OH vibrational frequency shift is also calculated and is close to the 60 cm^{-1} experimental value. A small amount of ozone is incorporated into the bulk and desorbs at the onset of the ice crystallization near 145 K.

I. Introduction

The simultaneous detection of H_2O and O_3 on an exoplanet is actually a topic of great importance[1] because it would be the signature of a biological process. On these planets, the O_3 production would be bound to the O_2 presence formed by a biological activity using water as solvent. However, recently, abiotic ozone, i.e., which is not formed by a biological process, was detected on Rhea and Dione, two satellites of Saturn[2] and on Ganymede a satellite of Jupiter.[3] This ozone would be induced by high-energy charged particle impacts or by photolysis of oxygen molecules that remain trapped in the water ice forming the surfaces of satellites.[4,2] Ozone is suspected to exist on voids that are localized on the surface of the ice.[2]

With regard to the pressure and temperature conditions which exist on these satellite surfaces (30 K, 10^{-8} mbar, for the dark faces of Rhea and Dione), it is reasonably expected that the ice is amorphous. More generally the amorphous ice is of great importance in the interstellar medium (ISM), mainly because it forms an icy mantle to the interstellar grains and this special medium is highly reactive.[5]

Infrared studies relative to O_3 adsorption on oxide surfaces such as SiO_2,[6] TiO_2,[7] Al_2O_3[8] have already been reported in the literature. These previous papers underlined the basicity of ozone which can form weak hydrogen bonds with surface OH groups via one of the terminal oxygen atoms. Other infrared[9] and microwave[10] experiments concerning the H_2O:O_3 complex have also shown the existence of a weak hydrogen bond between the two molecules.

The aim of the present work is to study, by FTIR spectroscopy, the adsorption of O_3 molecules on amorphous ice surface at low temperature under a low and constant pressure (10^{-7} mbar). Information on the nature of the adsorption sites can be derived from the experimental frequencies of O_3 and ice but also from the desorption activation energy measured by temperature-programmed desorption (TPD).[11,12] Moreover, TPD is a powerful method to determine the main desorption phases and thus the stability range of the molecule on the ice film.

Because the experimental methods give little information on the geometrical structure of the adsorption site, a quantum ab initio study was performed in order to analyze the nature of the interaction bonding O_3 to the ice surface.

II. Experimental Section

II.1. Ozone and Ice Sample Preparation, TPD Method. Ozone (O_3) was prepared from gaseous $^{16}O_2$ (Air Liquide N45, 99.995% pure) in an electric discharge and condensed in a tube cooled by liquid nitrogen. Residual oxygen was removed by secondary pumping. A small amount of pure ozone (<1 μmol) was deposited (at 1 μmol/min) on an amorphous ice film at 50 K, under a constant pumping of 10^{-7} mbar, to cover only the OH dangling and to avoid a solid sublayer formation.

Amorphous ice films were obtained from a water/argon (1/50) gaseous mixture deposited on a CsBr window held at 80 K with a 1 nm/s growth rate. The deposition is made under a constant pumping of 10^{-7} mbar in order to outgas Ar and so obtain a porous solid.[13] In addition, the use of a carrier gas allows a best control of the ice deposition. Then the film is recooled to 50 K to deposit O_3 and to study the adsorption process. The microporous[14] deposited films thickness is approximately of 0.1 μm as deduced from a calibration of infrared absorbance versus film thickness using optical interference.[15]

Adsorption and desorption of ozone on the amorphous ice film were monitored by infrared spectroscopy using a Nicolet 7199 FTIR spectrophotometer in the 4000−400 cm^{-1} wavenumber range at a resolution of 1 cm^{-1}.

Amorphous ice infrared spectra have been extensively described in the literature.[16,17] In addition to the bulk OH stretching and bending modes, they display a characteristic feature at 3695 cm^{-1} (Figure 1) which is relative to the OH stretching mode in which the H atom is not involved in hydrogen bonding. This mode, known as dangling OH mode according

* Author to whom correspondence should be addressed. E-mail: thierry@piimsdm3.univ-mrs.fr.

10.1021/jp001785y CCC: $20.00
Published on Web 12/21/2000

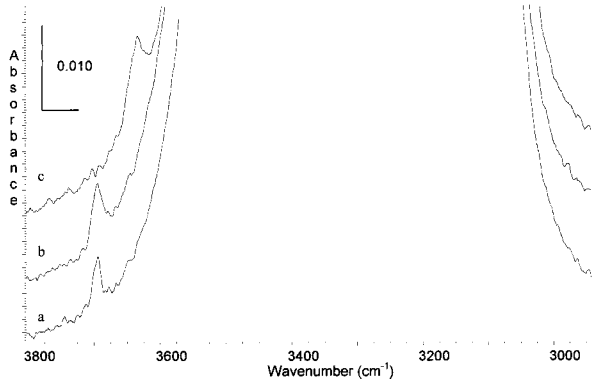

Figure 1. Dangling OH mode region during ozone exposure at different temperature. (a) Bare ice. (b) O_3 deposition at 25 K. (c) O_3 deposition at 45 K.

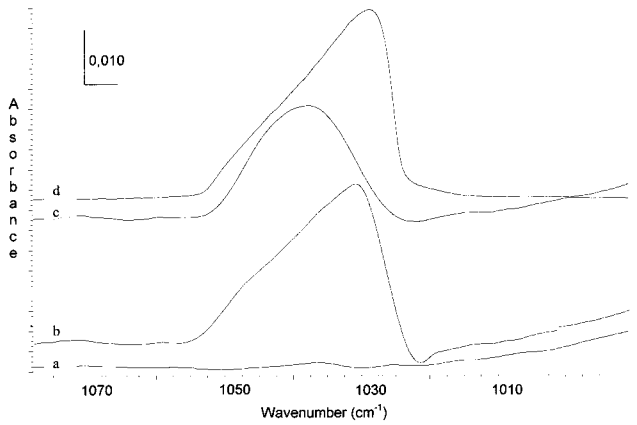

Figure 2. ν_3 mode of ozone during ozone exposure at different temperature. (a) Bare ice. (b) O_3 deposition at 25 K. (c) O_3 deposition at 45 K. (d) Solid O_3.

to Devlin, is assigned to 3-coordinated[18] water molecules existing both on the external surface and in the micropores of ice. This dangling bond is well-known to be an excellent probe to estimate the porosity[19,20] of the sample and also to follow the adsorption of molecules.[21−23] Since this dangling OH bond is enabled as proton donor[24,25] in hydrogen bond formation, it is a potential site for adsorption of proton acceptor molecules. Owing to its basic character, ozone is expected to be a proton acceptor.[8] However, we have to keep in mind that, on ice, these sites are not the only possible adsorption site, but that the lone pairs of electrons bearing O are also potential adsorption sites (dangling O in Devlin denomination[26]).

TPD is widely used to evaluate the adsorption energies[27] of different adsorption sites. As adapted to the FTIR spectroscopy,[28] this method consists of increasing the sample temperature and tracking the evolution of the main absorption band of ozone (i.e., the $\nu 3$ antisymmetric stretching mode). As desorption kinetics follow a first-order model, we can define the fractional surface coverage (θ) based on the following equation:[12]

$$\theta = \exp\left(\left(\frac{-A_d(T - T_0)}{\beta}\right)\exp\left(\frac{-E_d}{RT}\right)\right) \qquad (1)$$

where A_d is the first-order preexponential term, E_d the activation energy for desorption, R the gas constant, T the temperature, T_0 the temperature at which the desorption begins, and β the heating rate. The desorption rate at which the molecules leave the adsorption sites reaches a peak at the temperature T_p for which the second derivative of θ is equal to zero. From eq 1, this zero value leads to the relation:

$$\ln\left(\frac{\beta}{RT_p^2}\right) = -\frac{E_d}{RT_p} + \ln\left(\frac{A_d}{E_d}\right) \qquad (2)$$

and the mean values of E_d and A_d can be determined from eq 2 plotting $\ln(\beta/RT_p^2)$ versus $1/T_p$.

Several experiments were conducted using different β heating rates. For each of them we can evaluate the fractional surface coverage from the normalized integrated absorbance of the ozone $\nu 3$ mode versus T.

During a temperature increase for a TPD experiment, a modification of the ice surface occurs. Above 80 K we observed a reduction in the intensity of the dangling OH mode at 3695 cm^{-1} due both to a collapse of the pores and an ice restructuring. This behavior suggests an important dynamic surface reconstruction.[29−31] Moreover, in agreement with many authors,[32−34] we observed a transformation of the amorphous ice toward a crystalline form near 145 K. This irreversible transformation was monitored versus the temperature by the emergence of two shoulders[28] at 3340 and 3150 cm^{-1} on the large profile of the ν_{OH} mode at 3260 cm^{-1}. Ice retains its crystalline feature until the sample sublimates at 180 K.

II.2. Adsorption and Desorption of O_3 on Amorphous Ice Surface. Ozone adsorption on amorphous ice surface below 40 K induces a slight broadening but no change in the frequency position of the dangling OH mode (Figure 1b). The line shape of the ν_3 mode of O_3 at 1029 cm^{-1}, which is the more intense mode (Figure 2b), is the same as that observed for the solid O_3 directly deposited on the CsBr window (Figure 2d). Obviously, for temperatures below 40 K, we have deposited some solid ozone aggregates.

When ozone is deposited above 40 K, there appears a significant shift ($\Delta\nu_{OH} = \nu_{OH}$ (ice) $- \nu_{OH}$ (O_3-ice)) of the dangling OH group band to lower wavenumbers (Figure 1c). This result quite clearly demonstrates that O_3 diffusion occurs on the amorphous ice. Furthermore, the large shift of the dangling OH band, 60 cm^{-1}, indicates an interaction with the dangling OH groups. In the same time, an upshift of 7 cm^{-1} compared to the solid is observed for the ν_3 band (Figure 2c). The intensity of the shifted dangling OH band increases until all the dangling OH are saturated, for which it takes about 0.8 μmol of O_3. For our sample and at these temperatures, this amount of ozone introduced can be considered approximately as leading to the monolayer formation.

To identify the nature of the adsorption sites and to discriminate among the different adsorption sites evoked in the former section, we have coadsorbed gaseous O_3 and CF_4 on ice at 50 K. Due to its hydrophobic nature, CF_4 avoids the surface OH groups and associates strongly with the surface oxygen sites.[29] Moreover, at 50 K these molecules are mobile on the surface. The infrared spectrum analysis shows that the ozone ν_3 mode line shape (Figure 3b) is similar to that previously reported for O_3 deposited on ice without CF_4 (Figure 3a). This result indicates that each O_3 molecule interacts with OH groups of the ice surface.

After desorption of O_3, the dangling OH band which is restored in its original position (3695 cm^{-1}) has a weaker intensity than before O_3 exposure (Figure 4A). Considering that a residual band relative to the ν_3 mode of ozone remains constant in intensity from 90 K to near 145 K (Figure 4B), it can be concluded that an amount of O_3 is trapped into the bulk.

This was confirmed through two experiments. In the first one, O_3 is "sandwiched" between layers of amorphous ice. In the

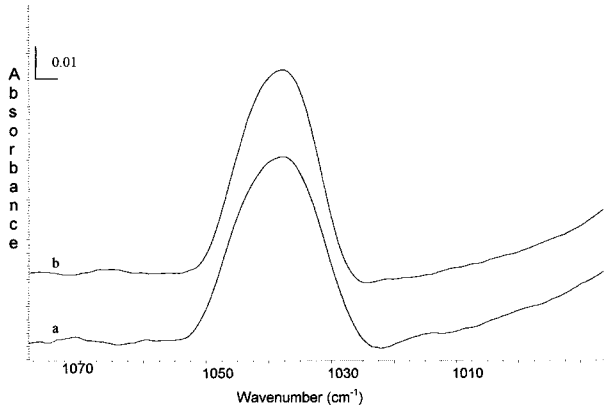

Figure 3. ν_3 mode of ozone. (a) Pure O_3 deposited at 50 K on an amorphous ice film. (b) O_3/CF_4 mixture deposited at 50 K on an amorphous ice film.

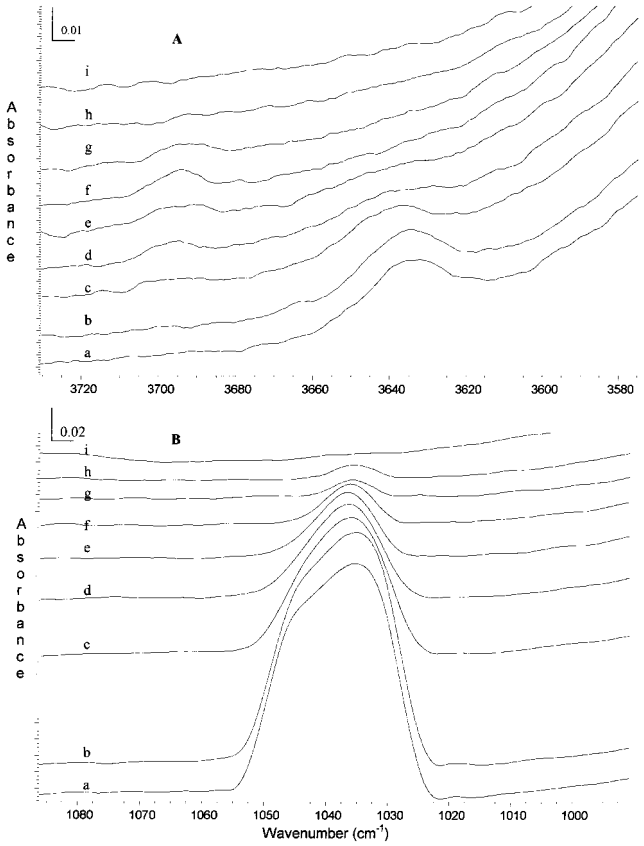

Figure 4. Selected infrared spectra during TPD ($\beta = 0.5$ K/min) of ozone from amorphous ice surface in the dangling OH mode region (A) and in the ν_3 mode region (B). (a) 50 K just after a deposition of 0.8 μmol of O_3; (b) 60 K; (c) 72 K; (d) 75 K; (e) 77 K; (f) 80 K; (g) 110 K; (h) 145 K; (i) 150 K.

second one, mixtures of O_3/H_2O are co-deposited. It is observed that in all cases, for a 0.5 K/min heating rate, the absorbed phase of O_3 disappeared completely near 145 K. This complete desorption of absorbed O_3 is induced by the onset of the ice crystallization from the amorphous ice film. This phenomenon has also been reported for other systems such as CCl_4,[35] acetone,[36] and C_3O_2.[28]

The O_3 desorption follows a first-order kinetic model as displayed in the linear plotting of $\ln \theta = f(T)$ in Figure 5A. To characterize the interaction energy between O_3 and amorphous ice surface we performed a TPD study monitored by infrared spectroscopy. Four experiments were conducted using different β (eqs 1 and 2) heating rates in the range 0.3 to 1 K/min. For

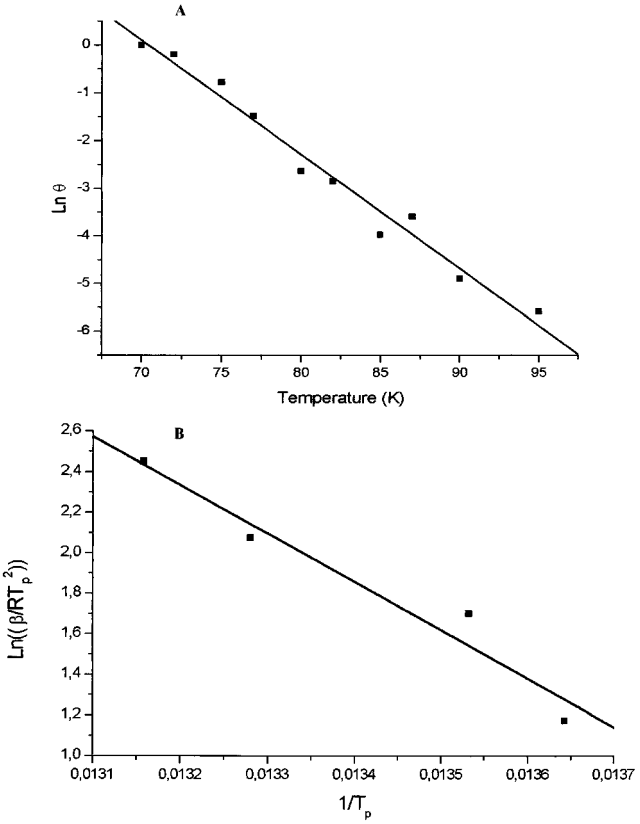

Figure 5. TPD results **(**A**)**: Experimental points of ln θ versus T for $\beta = 0.5$ K/min estimated through the integrated absorbance of the ν_3 mode of O_3 with its linear fit. **(B)**: Plot of $\ln(\beta/RT_p^2)$ versus $1/T_P$ for 4 TPD experiments with its linear fit.

TABLE 1: Desorption Peak Maximum Temperature (T_p) for Various β Heating Rates

β (K/min)	T_p (K)
0.3	73.3
0.5	73.9
0.7	75.3
1.0	76

each of them we observe that the integrated intensity of the ν_3 mode remains nearly constant between the deposition temperature (50 K) and T_0 defined in eq 1 equal to 70 K, where the O_3 molecules begin to desorb. Above this temperature a decrease of the ozone ν_3 mode (Figure 4B) and of the associated OH dangling mode at 3635 cm^{-1} is observed (Figure 4A). Meanwhile, free OH dangling mode increases in its original position at 3695 cm^{-1}. As a result, the temperature T_p is evaluated (Table 1) for each heating rate. From the linear plotting of $\ln(\beta/RT_p^2)$ versus $1/T_p$ (Figure 5B), $E_d = 20 \pm 3$ kJ/mol and $A_d = 4 \times 10^{11}$ s^{-1} are found. The uncertainty is derived from the standard deviation of the linear regression and this reflects the experimental uncertainty on T_p which is estimated at $\pm$ 0.5 K.

The TPD method is a routine method in the domain of surface sciences when coupled with mass spectrometry. It is, however, less frequently monitored by FTIR spectroscopy. From the above-described study, three important requirements can be deduced to make the results reliable.

(i) The temperature at which the adsorbed molecules become mobile must be evaluated: below this temperature, there is no molecular adsorption but rather deposition of aggregates.

(ii) The adsorption sites and their associated temperature range of stability must be carefully discriminated. In the case of O_3 adsorbed on amorphous ice, this process is achieved by CF_4 coadsorption in order to saturate the O type sites.

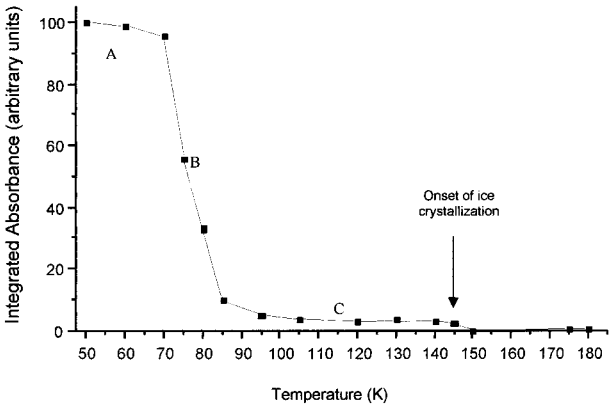

Figure 6. Normalized integrated absorbance of the ozone ν_3 mode versus temperature for ozone on ice surface. The temperature domains are denoted as (A) O_3 monolayer between 50 and 70 K, (B) desorption of O_3 between 70 and 90 K, (C) absorbed O_3 between 90 and 145 K.

(iii) The gaseous exposure must be stopped before formation of the adsorbate solid phase in order to avoid bulk effects.

These three requirements define the temperature domain where the TPD method is valid.

Taking account of these three statements and of the temperature domain of O_3 stability on amorphous ice (Figure 6), the TPD study was performed between 70 and 90 K (Figure 6, range B).

To complete these experiments, we have also deposited O_3 at 50 K on an annealed ice film at 165 K. Annealing affects the density and the porosity of ice;[37] this latter is much less porous than the amorphous ice films previously prepared. In this case, the temperature increase of the sample, with a heating rate of 0.5 K/min, reveals that no adsorption state is spectroscopically detected. Indeed we observe that O_3 totally sublimates at 70 K, as for pure solid O_3 directly deposited on CsBr window. This temperature is lower than for O_3 adsorbed on amorphous and non annealed ice film ($T \approx 90$ K).

III. Theoretical Section

III.1. Method of Calculation. The periodic Hartree−Fock method[38] (PHF) has been widely used in our earlier works and proved to be very powerful to determine the adsorption site structure and the associated energy for various systems such as CO,[39] C_2H_2,[40] HCl, C_3O_2.[41] The general strategy remains unchanged in the present paper except that we extended the study to the shift of the dangling OH mode frequency induced by the O_3 adsorption process.

As previously stated, the ice is represented by a slab of infinite 2D layers corresponding to the structure optimized by Pisani et al.[38] using the PHF method and CRYSTAL98.[42] The orbital basis set is 6-31g** which already proved to be well adapted. The problem of the basis set completeness is corrected by the usual counterpoise method.[43] The optimization procedure concerns both the adsorbed O_3 molecule and the water molecule bearing the dangling OH moiety.

As stated also in our previous papers[39,41] the quantum study of adsorption on ice can be handled by two types of ab initio methods: the cluster model deals with a very restricted number of water molecules, thus it is unable to reproduce with enough accuracy the cooperative and collective effects of the hydrogen bonds in ice. On the other side PHF model takes into account these effects very efficiently.[44] The counterpart is that the surface is represented as perfectly ordered. However one of the major conclusion of one of our previous paper[39] was that at the molecular scale, it can be considered that the adsorbate environment is partly ordered. The so-called amorphous ice must not be considered as a real glass, the constitutive patterns of ice remains identifiable: hydrogen bonds network, 6-molecules rings, tetrahedral organization.... The surface disorder is induced by deformation of the O−O−O angles (about 14° following Devlin et al.[45]) or of the tetrahedral angles. Nevertheless in the special case of ozone adsorption the cluster model failed to give the good order of magnitude for the vibrational shift whereas the PHF method gives a good semiquantitative description of the phenomenon.

TABLE 2: O_3 Geometrical Parameters Obtained by Different Methods of Calculation with a DZP Basis Set from Ref 49

	this work pw91	CASSF	CCSD	CCSD(T)	CISD(TQ)	expt
R (Å)	1.283	1.296	1.263	1.287	1.281	1.272
α (°)	117.9	116.5	117.4	116.8	116.7	116.8

Since the energy gradient calculation is not included into the CRYSTAL98 package, the energy minimum is determined by successive quadratic interpolation. At each point the HF energy is corrected by the electronic correlation contribution. The correlation energy is calculated by the density functional method (DFT) using the nonlocal gradient corrected functional determined by Perdew et al.[46] (GGA).

At minimum the adsorption energy is calculated as

$$\Delta E_a = (E_{ice} + E_{ozone}) - E_{ice + ozone}$$

where each term is evaluated using the entire orbital set as usual in the Boys's method.[43]

The dangling OH vibration frequency is very sensitive to any modification of the ice surface because it belongs to a domain of the surface where the electric fields generated by the substrate and the adlayers are very strong.[44] One of the major effect of this environment is to decouple the stretching OH modes. One of the hydroxyls is tightly entangled in the bulk OH modes by its hydrogen bond, whereas the dangling OH is only submitted to the surface electrostatic field. It can be possibly coupled to its first equivalent in the neighborhood of a unit cell at a distance of 4.4 Å in our model: this coupling is therefore weak.

As a consequence, the dangling OH vibration mode can be considered as a local mode embedded in the field resulting from the ice, combined to the field generated by the O_3 adsorbate. Thus, concerning this typical vibrational mode, the quantum calculation can be restricted to this well-defined water molecule.

The Wilson generalized valence force field[47] is calculated in internal coordinates by the method of finite elements[48] at the same level of theory as before.

III.2. Quantum Results. The potential energy surface and harmonic force field of the O_3 molecule has received a great deal of attention in recent years.[49] Most of the theoretical calculations have been developed within multi-configuration methods,[50] many body perturbation theories,[51] coupled cluster methods[52] or configuration interaction.[53] However these methods are not applicable in the domain of the solid state and the starting point of the O_3 configuration is provided by a DFT gradient corrected Perdew-Wang 91[46] calculation using the same orbital basis set as in CRYSTAL98. The structure so calculated is compared to more sophisticated calculations in Table 2. Concerning the O−O bond length the DFT result is quite similar even to the very sophisticated Leininger et al.[49] calculations. The main discrepancy concerns the angle, the DFT value is too large compared to experiment but of the same order of magnitude as the CCSD calculations.

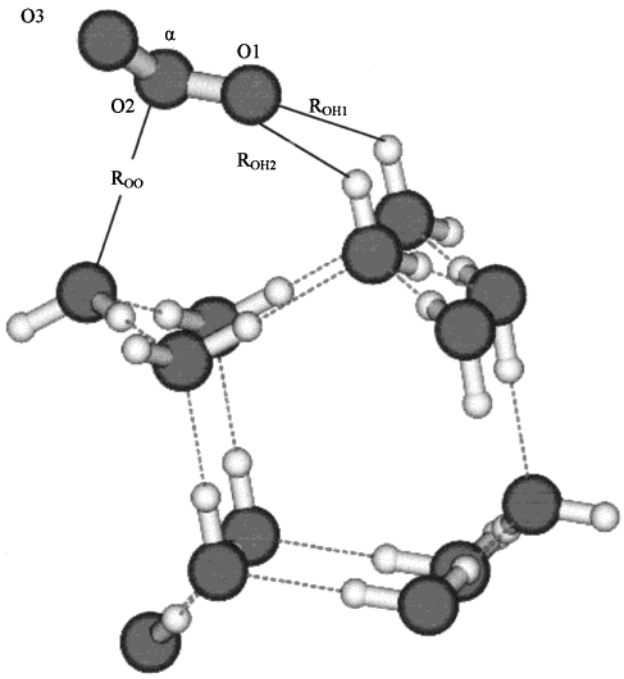

Figure 7. Optimized geometry of ozone molecules adsorbed on ice. For comparison, the experimental values are given for isolated O_3 excepted for the ΔE value that corresponds to the desorption energy obtained by TPD.

TABLE 3: Geometrical Parameters (as labeled in Figure 6) of Isolated O_3 and Adsorbed O_3 on Ice Obtained by PHF/6-31 g Calculation Followed by a GGA Correction of the Correlation Energy**

	isolated O_3	expt	adsorbed O_3
R_{O1O2} (Å)	1.283	1.272[a]	1.193
R_{O2O3} (Å)	1.283	1.272[a]	1.186
α (°)	117.9	116.8[a]	118.8
R_{OO} (Å)			3.001
R_{OH1} (Å)			2.348
ΔE (kJ/mol)		20 ± 3[b]	15

[a] From ref 49. [b] This work.

TABLE 4: Mulliken's Charges of Isolated O_3 and Adsorbed O_3 on Ice Obtained by PHF/6-31 g Calculation Followed by a GGA Correction of the Correlation Energy**

	isolated O_3	adsorbed O_3
O1	−0.105	−0.212
O2	0.210	0.365
O3	−0.105	−0.147

In the adlayer, the ozone molecule lies on the surface as shown in Figure 7 and detailed in Table 3. The stability of the system is ensured by a weak hydrogen bond with the nearest dangling OH ($d_{O...H}$ = 2.348 Å) and by electrostatic interaction. The adsorption energy corrected from the BSSE is 15 kJ/mol, which is in good agreement with the desorption energy determined through the TPD method (20 ± 3 kJ/mol).

The adsorption process induces a disymmetry into the adsorbed molecule. The H bonded O−O is longer due to an effect of cooperativity of the hydrogen bonds but the two bond lengths are noticeably shorter than for the isolated molecule. This result is in good agreement with the high-field shift generally observed for the stretching mode frequency induced by adsorption. On the contrary, the angle value remains unchanged.

The surface field causes a sharper polarization of the O_3 electrons density since the Mulliken populations analysis evidences a transfer from the central oxygen to the other two, overall toward the H-bonded one.

The dangling OH local mode harmonic frequency calculated as described in the former section is 3611 cm^{-1} after scaling by a standard factor of 0.85. The equivalent frequency calculated by the same method for the neat ice surface is 3692 cm^{-1}. The PHF/DFT calculated frequency is then shifted by 81 cm^{-1} toward the lower fields. The experimental shift is observed in the same direction and its value is 60 cm^{-1}, therefore our method of calculation provides both the correct sign and the correct order of magnitude. The approximations to be made are certainly responsible for the difference between the two numerical values. However, we have also to keep in mind that the theoretical value is harmonic, whereas the experimental one certainly is not. However, the quantum calculation shows that the frequency shift is very large compared to a small interaction energy between the admolecule and the surface. Therefore, this shift must rather be related to the electric field perturbation of the neighborhood of the dangling OH and then probably to the admolecule polarizability.[53]

IV. Discussion and Conclusion

The analysis of the ozone $\nu 3$ mode integrated absorbance (Figure 6) shows that O_3 in a monolayer state desorbs in the 70−90 K range temperature. However, there remains a small amount of O_3 which gets trapped into the bulk from 90 to 145 K. Absorbed O_3 could be explained through the dynamic character of the ice surface which can occur even for $T < 90$ K according to Laufer et al.[30,31] The ice surface relaxation leads to a reduction of the porosity and the latter can be correlated to a decrease of the dangling OH band intensity as the temperature is higher than 80 K.[37] So, as the pores are closing, ozone is embedded. From our experiments, we can see that around 5−10% of the global deposited ozone is embedded in the ice bulk. However, when O_3 is deposited on an annealed ice film and so less porous, it is not trapped.

It is remarkable that this absorbed phase of ozone desorbs at the onset of ice crystallization. This desorption probably occurs during the nucleation and growth of crystalline ice from amorphous water via a dynamic percolation mechanism as reported by Kay an co-workers.[35]

According to the periodic Hartree−Fock study, O_3 interacts weakly with the surface. This interaction occurs via two types of electrostatic interactions (Figure 7). The first is relative to the lone pairs of electrons bearing O of a water molecule with the central oxygen of ozone, and the second is due to the dangling OH of another water molecule with a lateral oxygen of ozone. The calculated adsorption energy (ΔE_a= 15 kJ/mol) and the calculated dangling OH frequency shift ($\Delta \nu_{OH}$ = 80 cm^{-1}) are in the same order of magnitude as the experimental data: desorption activation energy (E_d = 20 ± 3 kJ/mol) and frequency shift (60 cm^{-1}). These two tests, concerning not only the energy but also the second derivative of energy, ensure a good degree of reliability to the quantum study, and this despite the fact that the PHF model implies a perfect ice surface. This result implies that this study supports the Knözinger et al.[55] interpretation of X-ray diffraction experiments showing that the porous ice surface presents a short-range local order, which also was the conclusion of one of our earlier papers.[39]

The present study shows that O_3 stability temperature range on ice occurs below 90 K and it is consistent with interstellar medium conditions ($T < 150$ K). The study results are consistent with the fact that O_3 was detected on satellites of Jupiter and Saturn[2−4] by Hubble Space Telescope. However, O_3 has never

been detected directly in interstellar icy grain. This is probably due to the fact that $\nu 3$ band of ozone is obscured by the strong and broad absorption band of silicates[56] which made up these grains. Moreover, it is well-known that ozone leads, even at very low temperature, to a great chemical[57] and photochemical[58] reactivity. Therefore, there could be an interstellar ozone reactivity which also involves the interstellar ice either as catalyst[5] or as reagent.[59] But this domain is still largely unexplored.

References and Notes

(1) Léger, A.; Ollivier, M.; Altwegg, K.; Woolf, N. J. *Astron. Astrophys.* **1999**, *341*, 304.
(2) Noll, K. S.; Roush, T. L.; Cruikshank, D. P.; Johnson, R. E.; Pendleton, Y. J. *Nature* **1997**, *388*, 45.
(3) Noll, K. S.; Johnson, R. E.; Lane, A. L.; Domingue, D. L.; Weaver, H. A. *Science* **1996**, *273*, 341.
(4) Hunten, D. M. *Nature* **1995**, *373*, 654.
(5) Tamburelli, I.; Chiavassa, T.; Borget, F.; Pourcin, J. *J. Phys. Chem. A* **1998**, *102*, 423.
(6) Bulanin, K. M.; Alexeev, A. V.; Bystrov, D. S.; Lavalley, J. C.; Tsyganenko, A. A. *J. Phys. Chem.* **1994**, *98*, 5100.
(7) Bulanin, K. M.; Lavalley, J. C.; Tsyganenko, A. A. *J. Phys. Chem.* **1995**, *99*, 10294.
(8) Thomas, K.; Hoggan, P. E.; Mariey, L.; Lamotte, J.; Lavalley, J. C. *Catal. Lett.* **1997**, *46*, 77.
(9) Schriver, L.; Barreau, C.; Schriver, A. *Chem. Phys.* **1990**, *140*, 429.
(10) Gillies, J. Z.; Gillies, C. W.; Suenram, R. D.; Lovas, F. J.; Schmidt, T.; Cremer, D. *J. Mol. Spectrosc.* **1991**, *146*, 493.
(11) Readhead, P. A. *Vacuum* **1962**, *12*, 203.
(12) Yates, J. T. *Methods Exp. Phys.* **1985**, *22*, 425.
(13) Givan, A.; Loewenschuss, A.; Nielsen, C. J. *J. Phys. Chem. B* **1997**, *101*, 8696; Givan, A.; Loewenschuss, A.; Nielsen, C. J. *Chem. Phys. Lett.* **1997**, *275*, 98.
(14) Mayer, E.; Pletzer, R. *Nature* **1986**, *319*, 298.
(15) Zondlo, M. A.; Onash, T. B.; Warshavsky, M. S.; Tolbert, M. A.; Mallich, G.; Arentz, P.; Robinson, M. S. *J. Phys. Chem. B* **1997**, *101*, 10887.
(16) Rowland, B.; Devlin, J. P. *J. Chem. Phys.* **1991**, *94*, 812.
(17) Buch, V.; Devlin, J. P *J. Chem. Phys.* **1999**, *110*, 3437, and references herein.
(18) Buch, V.; Devlin, J. P. *J. Chem. Phys.* **1991**, *94*, 4091.
(19) Givan, A.; Loewenschuss, A.; Nielsen, C. *Vib. Spectrosc.* **1996**, *12*, 1.
(20) Rowland, B.; Kadagathur, N. S.; Devlin, J. P. *J. Chem. Phys.* **1991**, *94*, 4091.
(21) Devlin, J. P. *Physics and chemistry of ice*; Maeno and Hondo: Sapporo, 1992; p 183.
(22) Rowland, B.; Kadagathur, N. S.; Devlin, J. P.; Buch, V.; Feldman, T.; Wojcik, M. J. *J. Chem. Phys.* **1995**, *102*, 8328.
(23) Schaff, J. E.; Roberts, J. T. *J. Phys. Chem.* **1996**, *100*, 1451.
(24) Schaff, J. E.; Roberts, J. T. *J. Phys. Chem.* **1994**, *98*, 6900.
(25) Roberts, J. T. *Acc. Chem. Res.* **1998**, *31*, 415.
(26) Devlin, J. P.; Buch, V. *J. Phys. Chem. B* **1997**, *101*, 6095.
(27) Smith, R. S.; Huang, C.; Wong, E. K. L.; Kay, B. *Surf. Sci.* **1996**, *367*, L13.
(28) Couturier-Tamburelli, I.; Chiavassa, T.; Pourcin, J. *J. Phys. Chem. B* **1999**, *103*, 3677.
(29) Devlin, J. P. *J. Phys. Chem.* **1992**, *96*, 6185.
(30) Bar-Nun, A.; Dror, J.; Kochavi, E.; Laufer, D. *Phys. Rev. B* **1987**, *35*, 2427.
(31) Laufer, D.; Kochavi, E.; Bar-Nun, A. *Phys. Rev. B* **1987**, *36*, 9219.
(32) Narten, A. H.; Venkatesh, C.; Rice, S. A. *J. Chem. Phys.* **1976**, *64*, 1106.
(33) Jenniskens, P.; Blake, D. F. *Science* **1994**, *265*, 273.
(34) Jenniskens, P.; Blake, D. F.; Wilson, M. A.; Pohorille, A. *Astrophys. J.* **1995**, *455*, 389.
(35) Smith, R. S.; Huang, C.; Wong, E. K. L.; Kay, B. D. *Phys. Rev. Lett.* **1997**, *79*, 5.
(36) Schaff, J. E.; Roberts, J. T. *Langmuir* **1998**, *14*, 1478.
(37) Berland, B. S.; Brown, D. E.; Tolbert, M. A.; George, S. M. *Geophys. Res. Lett.* **1995**, *22*, 3493.
(38) Pisani, C.; Canassa, S.; Ugliengo, P. *Chem. Phys. Lett.* **1996**, *253*, 201.
(39) Allouche, A.; Verlaque, P.; Pourcin, J. *J. Phys. Chem. B* **1998**, *102*, 89.
(40) Allouche *J. Phys. Chem. A* **1999**, *103*, 9150.
(41) Allouche, A.; Couturier-Tamburelli, I.; Chiavassa, T. *J. Phys. Chem. B* **2000**, *104*, 1497.
(42) Saunders, V. R.; Dovesi, R.; Moetti, C.; Causa, M.; Harrison, N. M.; Orlando, R.; Zicovich-Wilson, C. M. *CRYSTAL98 user's manual*; Università di Torino.
(43) Boys, S. F.; Bernardy, F. *Mol. Phys.* **1970**, *19*, 553.
(44) Manca, C.; Allouche, A. *J. Chem. Phys.* **2001**, in press.
(45) Devlin, J. P.; Joyce, C.; Buch, V. *J. Phys. Chem. A* **2000**, *104*, 1974.
(46) Perdew, J. P.; Wang, Y. *Phys. Rev. B* **1986**, *33*, 8800.
(47) Califano, S. *Vibrational States*; John Wiley: London, 1967.
(48) Allouche, A.; Cora, F.; Girardet, C. *Chem. Phys.* **1995**, *201*, 59.
(49) Leininger, M. L.; Schaeffer, H. F. *J. Chem. Phys.* **1997**, *107*, 9059, and references herein.
(50) Yamaguchi, Y.; Frish, M. J.; Lee, T. J.; Schaeffer, H. F.; Binkley, J. S. *Theor. Chim. Acta* **1986**, *69*, 337; Alder-Golden, S. M.; Langhoff, S. R.; Banschlisher, C. W.; Carney, G. D. *J. Chem. Phys.* **1985**, *83*, 255.
(51) Stanton, J. F.; Limpscomb, W. N.; Majers, D. H.; Bartlett, R. J. *J. Chem. Phys.* **1989**, *90*, 1077.
(52) Majers, D. H.; Bartlett, R. J.; Stanton, J. F. *J. Chem. Phys.* **1989**, *91*, 1945.
(53) Lee, T. J.; Allen, W. D.; Schaeffer, H. F. *J. Chem. Phys.* **1987**, *87*, 7062.
(54) Holmes, N. S.; Sodeau, J. R. *J. Phys. Chem. A* **1999**, *103*, 4673.
(55) Langel, W.; Fleger, H.-W.; Knözinger, E. *Ber. Bunsen-Ges. Phys. Chem.* **1994**, *98*, 81.
(56) Ehrenfreund, P.; Breukers, R.; d'Hendecourt, L.; Greenberg, J. M. *Astron. Astrophys.* **1992**, *260*, 431.
(57) Samuni, U.; Fraenkel, R.; Haas, Y.; Fajgar, R.; Pola, J. *J. Am. Chem. Soc.* **1996**, *118*, 3687.
(58) Bahoo, M.; Schriver-Mazzuoli, L.; Camy-Peyret, C.; Schriver, A.; Chiavassa, T.; Aycard, J. P. *Chem. Phys. Lett.* **1997**, *265*, 145.
(59) Sedlacek, J.; Wight, C. A. *J. Phys. Chem.* **1989**, *93*, 509.